



Journal of Advanced Research in Fluid Mechanics and Thermal Sciences

Journal homepage:

https://semarakilmu.com.my/journals/index.php/fluid_mechanics_thermal_sciences/index

ISSN: 2289-7879



Heat Transfer Analysis on Peristaltic Transport of Sisko Fluid in an Inclined Uniform Channel

Prathiksha Sanil¹, Manjunatha Gudekote^{1,*}, Rajashekhar Choudhari², Hanumesh Vaidya³, Kerehalli Vinayaka Prasad³

¹ Department of Mathematics, Manipal Institute of Technology, Manipal Academy of Higher Education, Manipal, Karnataka, India

² Department of Mathematics, Manipal Institute of Technology, Bengaluru Campus, Manipal Academy of Higher Education, Karnataka, India

³ Department of Mathematics, Vijayanagara Sri Krishnadevaraya University, Ballari, Karnataka, India

ARTICLE INFO

Article history:

Received 28 October 2022

Received in revised form 5 February 2023

Accepted 13 February 2023

Available online 25 February 2023

Keywords:

Sisko fluid; slip condition; inclined channel; fluid behaviour index; variable fluid properties

ABSTRACT

Peristaltic flow is a fundamental method of fluid conveyance in engineering, medicine, and the nuclear industry. The peristaltic mechanism is applied in designing blood pump machines, dialysis machines, and other medical devices. The current mathematical model is developed to investigate the peristaltic mechanism of Sisko fluid under the influence of heat transfer by considering variable viscosity, slip effects, variable thermal conductivity, and wall properties. Long wavelength and small Reynolds number approximations generate the nonlinear governing equations. The regular perturbation method is utilised to solve these equations. In contrast, the closed-form solution is obtained for the stream function for different values of the fluid behaviour index. The impact of several parameters on the relevant physiological factors is graphically represented using MATLAB. The results reveal that velocity and thermal slip parameters greatly impact heat transfer. The bolus volume grows as the velocity slip parameter increases. The coefficient of pseudo-plasticity plays a prominent role in the study for different values of fluid behaviour index.

1. Introduction

Peristalsis is a fluid conveyance caused by a gradual wave of expansion or contraction along the walls of a liquid-filled distensible duct. It is employed in a wide range of biomedical and biological systems. It is crucial to many processes in physiology, including the flow of chyme in the gi-tract, the mobility of seminal fluid in the ductus efferents of male reproductive tracts, the movement of the embryo in female oviduct, and the cardiovascular system. Numerous theoretical and empirical studies have been conducted to comprehend peristalsis. Earlier studies on peristaltic motion were executed by considering Newtonian fluid. The mechanism of peristalsis was first initiated by Latham [1] in understanding the urine flowing through ureter. Shapiro *et al.*, [2] used a low Reynolds number and long wavelength assumption to study peristaltic pumping. For the amplitude ratios ranging from

* Corresponding author.

E-mail address: manjunatha.g@manipal.edu

<https://doi.org/10.37934/arfmts.103.2.157179>

zero to complete occlusion, theoretical conclusions are presented for plane and axisymmetric geometries. The theoretical parameters were validated in a quasi-two-dimensional apparatus experiment. However, due to their broader application in complex structures and the dual behaviour of blood, non-Newtonian fluids have been used in recent studies. Raju and Devanathan [3] initiated a study investigating the peristalsis of non-Newtonian fluids under various geometrical conditions. A power series in terms of wave amplitude is used to calculate the stream function's solution. Many researchers have recently conducted numerous studies by considering different conditions [4-6].

In addition, many researchers have given more importance to the slip effects on biological fluids. It has a particular interest of active researchers due to its application in technology and medicine. Slip flow is more appropriate than no-slip flow in various fluid flow scenarios. The liquid exhibits a decline in adherence at the wet wall surface in numerous applications, resulting in a slip flow, which causes the liquid to slide along the walls. When studying the interactions between fluids and solid surfaces, the idea of the slip flow of a liquid at a solid wall is crucial in explaining the macroscopic consequences. Most peristaltic flow studies do not take the slip effect into account. Considering this, the impact of slip and varying viscosity on non-Newtonian fluid flow through permeable media in an inclined channel was investigated by Khan *et al.*, [7] by applying the traditional perturbation approach to solve the system of the nonlinear governing equation. The key characteristics of the pumping and trapping processes are thoroughly described. The flow is studied in a wave frame of reference that moves with the wave's velocity. As of late, in a porous inclined elastic tube, Gudekote *et al.*, [8,9] examined the influence of slip effects on the peristaltic motion of Casson fluid. According to their study, the pressure rise increases accordingly with a rise in the inclination angle. Additionally, the pressure rise is significantly reduced as the porosity increases [8]. Likewise, a higher value for the variable viscosity and porosity parameters expands the trapped bolus's size, promoting boluses' development [9]. The slip effects on a peristaltic motion for non-Newtonian fluid have also been discussed by Prasad *et al.*, [10]. Graphs are drawn to examine and describe the impact of essential variables on physical quantities. The current flow data show some fascinating phenomena relevant to the biomedical field. In recent days, the effect of velocity slip and thermal slip on the peristalsis flow of a Herschel-Bulkley liquid via an inclined porous tube was investigated by Baliga *et al.*, [11]. The results show that thermal and velocity slip impacts pressure rise and temperature increase with time. It is noticed that as the velocity slip parameter increases, the bolus volume also does. Recently Balachandra *et al.*, [12] examined the slip effects and varying liquid properties on a Ree-Eyring fluid peristaltic transport through a channel with inclination. The analysis demonstrates that the slip parameter and variable viscosity cause the development of the velocity profiles. The liquid parameter also controls the size of the trapped bolus. The results also help in identifying the blood flow in tiny arteries. Khan and Wang [13] investigated the effects of peristaltic non-Newtonian incompressible particulate fluid flow involving identical rigid particles distributed uniformly in a channel using electro magnetohydrodynamics. Slip boundary conditions of the second order are also employed.

Peristalsis and heat transfer interaction plays a crucial role and has several applications. In the human body, heat transport is currently recognised as an important area for research. Hence such analysis is critical. Thermotherapy and thermoregulation strategies have inspired biomedical engineers to study tissue bioheat transport. The importance of thermophysical qualities in comprehending diverse bodily functions has come to the attention of researchers in recent years. Until recently, peristaltic flow research assumed that thermo-physical parameters were stable during the blood flow. However, the temperature and velocity are observed to change, as in the case of blood. These characteristics vary in physiological liquids. Including viscosity and heat conductivity is essential when considering the variance in both properties. As a result, considering these effects becomes critical. Vajravelu *et al.*, [14] studied the influence of heat transmission on the peristaltic

movement through the permeable annulus. Rajashekhar *et al.*, [15] examined the peristaltic movement of Casson fluid in an inclined porous tube. It was seen that rising variable viscosity improves the velocity and the temperature of the liquid and enhances the bolus size. Vaidya *et al.*, [16,17] examined the influence of variable fluid properties on Rabinowitsch with different geometries under various conditions. Based on the data, thermal and velocity slip impacts velocity, and slip parameters substantially affect the flow quantities of Newtonian, dilatant and pseudoplastic fluid models. The analysis also demonstrates that the occurrence of the trapping phenomena is enhanced by rising the value of porous characteristics and variable viscosity [16]. Similarly, the results show that as the porosity parameter increases, the velocity rises for Newtonian and shear-thinning fluids but diminishes for shear-thickening fluids [17]. Additionally, it can be seen that Biot number raises the temperature for dilatant liquids, whereas it lowers for Pseudoplastic and Newtonian fluids. In a non-uniform channel with porous walls, Manjunatha *et al.*, [18] examined the peristalsis of Jeffery fluid under the effects of variable liquid properties. The analysis reveals that increasing the variable viscosity improves the temperature, Nusselt number, and velocity fields, while concentration profiles exhibit the opposite behaviour. Additionally, a rise in the porosity and Jeffery parameter values is observed, along with increased trapped bolus volume. Khan *et al.*, [19] analysed the variable properties of viscosity and thermal conductivity in the peristalsis of a magneto-Carreau nanofluid with heat transfer. Compared to viscous nanomaterial and steady viscosity, Carreau nanomaterial and variable viscosity have a higher velocity. For varying thermal conductivity, temperature and concentration of nanomaterials have opposing responses. Abuiyada *et al.*, [20] examined MHD peristaltic transfer of Bingham nanofluid by considering Soret and Dufour effects. The increasing velocity slip parameter was found to increase the velocity, but near the right wall of the channel, the behaviour reverses. Vaidya *et al.*, [21] examined the peristaltic motion of Phan-Thien-Tanner fluid via a non-uniform axisymmetric inclined channel by considering wall properties. Convective boundary conditions and the effects of chemical reactions are investigated. It was discovered that varying thermal conductivity could help regulate the liquid temperature.

Due to their numerous practical applications, peristaltic flows of non-Newtonian Sisko fluids have recently allured the particular attention of researchers. Wang *et al.*, [22] investigated the magnetohydrodynamics peristaltic mechanism of a Sisko fluid in an asymmetric channel. Sisko fluids that exhibit shear-thinning and shear-thickening behaviours are studied and compared to Newtonian fluids. The investigation is conducted about various material properties and the differences in the wall peristalsis phase, including velocity distributions, shear stress, pressure gradients, and streamline patterns. Further, Nadeem and Akbar [23] studied the peristalsis of Sisko fluid in a uniform inclined tube. The different physiological interests, such as frictional force, pressure rise, pressure gradient and trapping phenomena, have been calculated numerically with other physical parameters. Analytical and Numerical solutions on the Peristaltic flow of a Sisko fluid in an endoscope were done by Nadeem *et al.*, [24]. Further, Mehmood and Fetecau [25] observed that factors such as buoyancy and radiation augment the pumping and trapping phenomenon when studying the impact of radiative heat transmission with varying wall temperatures in an asymmetric channel on the Sisko fluid peristaltic flow. Malik and Khan [26] conducted a numerical analysis of homogeneous-heterogeneous responses in the Sisko fluid flow field across an extending cylinder. The study claims concentration profiles diminish for increasing homogeneous and heterogeneous reaction parameter values. Tanveer *et al.*, [27] investigated the impact of varying viscosity on the Sisko fluid peristalsis in a curved conduit with compliant wall properties. The corresponding equations are solved using perturbation and numerical approaches to achieve qualitatively equivalent responses for both velocity and temperature. It was found that the Sisko fluid parameter decreases the temperature and velocity profiles. Asghar *et al.*, [28] analysed the non-Newtonian Sisko fluid in an oscillating porous

curved channel during peristalsis. Compared to the power-law and Newtonian models, the Sisko model predicts greater velocity values in the central core region of the flow. Iqbal *et al.*, [29] studied the peristalsis of Sisko fluid in an asymmetric channel. The study focuses on the shear-thickening and shear-thinning properties of the Sisko fluid. The distributions of velocity and temperature, as well as the pressure gradient and streamline pattern, are investigated. Consequently, the thermal analysis indicated that raising a non-Newtonian parameter, such as the Brinkman numbers and Biot number, enhances the thermal stability of the liquid. The peristaltic flow of the non-Newtonian Sisko fluid model under the combined effects of MHD and slip in a symmetric channel is investigated by Imran *et al.*, [30]. It is observed that increasing the value of the Sisko parameter reduces the momentum distribution. The blood velocity can be controlled by varying the intensity of the magnetic field. The peristaltic motion of electrically conducting Sisko fluid in a non-symmetric porous tapered tube with velocity slip condition was explored by Abbas *et al.*, [31] in the presence of chemical reactions. To simulate the effect of permeability, modified Darcy's law was used. Thermal radiation and viscous dissipation were also considered.

The current study is inspired by the abovementioned research and predicts the effects of variable liquid properties on the peristaltic transport of Sisko fluids in an inclined channel. This aspect of the study has yet to be thoroughly examined. The study provides a semi-analytical approach to solving nonlinear systems with slip conditions. The long wavelength and low Reynolds number assumptions are considered. Convective boundary conditions and slip conditions have also been studied for heat transfer. Graphs illustrate the effect of pertinent parameters on physiological quantities while under the supervision of measurable criteria. Potential applications of this idea exist in the area of medicine.

2. Mathematical Formulations

Consider the peristaltic transport of a viscous incompressible Sisko fluid flowing through a uniform channel. The sinusoidal wave trains of wavelength λ propagating with speed c , cause the fluid motion along the channel walls.

Geometry of the uniform channel (Figure 1) given by the expression

$$H' = a' + b' \sin \left[\frac{2\pi}{\lambda} (z' - ct') \right] \tag{1}$$

where H' is the uniform wave in which a' is the uniform radius, b' is the wave amplitude, and t' is the time.

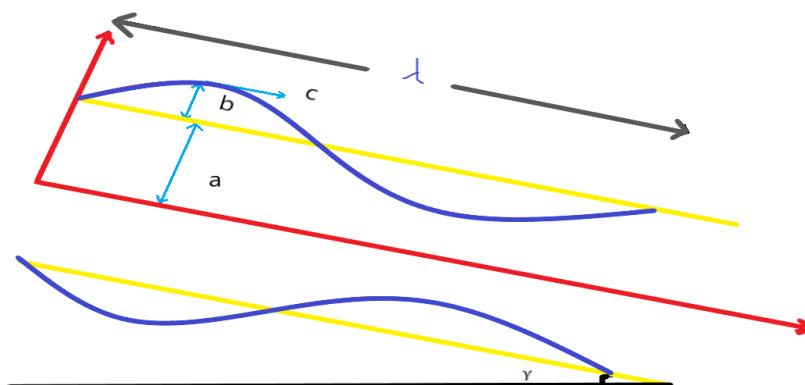


Fig. 1. Geometry of the uniform channel

For a Sisko fluid flow, the equation of continuity, equation of motion and energy equation are written as

$$\frac{\partial u'}{\partial x'} + \frac{\partial w'}{\partial y'} = 0 \quad (2)$$

$$\rho \left[\frac{\partial w'}{\partial t'} + u' \frac{\partial u'}{\partial x'} + w' \frac{\partial u'}{\partial y'} \right] = -\frac{\partial p'}{\partial x'} + \frac{\partial \tau'_{x'x'}}{\partial x'} + \frac{\partial \tau'_{x'y'}}{\partial y'} + \rho g \sin \gamma \quad (3)$$

$$\rho \left[\frac{\partial w'}{\partial t'} + u' \frac{\partial w'}{\partial x'} + w' \frac{\partial w'}{\partial y'} \right] = -\frac{\partial p'}{\partial x'} + \frac{\partial \tau'_{x'x'}}{\partial x'} + \frac{\partial \tau'_{y'y'}}{\partial y'} + \rho g \cos \gamma \quad (4)$$

$$\rho C_p \left[\frac{\partial T'}{\partial t'} + u' \frac{\partial T'}{\partial x'} + w' \frac{\partial T'}{\partial y'} \right] = k_1 \left[\frac{\partial^2 T'}{\partial x'^2} + \frac{\partial^2 T'}{\partial y'^2} \right] + \tau'_{x'x'} \frac{\partial u'}{\partial x'} + \tau'_{y'y'} \frac{\partial w'}{\partial x'} + \tau'_{x'y'} \left(\frac{\partial u'}{\partial x'} + \frac{\partial w'}{\partial x'} \right) \quad (5)$$

where u' , w' are velocity components in radial and axial directions respectively. ρ is fluid density, p' is pressure, $\tau'_{x'x'}$, $\tau'_{x'y'}$, $\tau'_{y'y'}$ are extra stress components, while k_1 , T' , C_p denotes mass diffusivity coefficient, temperature and the specific heat at constant volume respectively.

Convective boundary conditions for the problem are given as follows

$$\frac{\partial w'}{\partial y'} = \tau_0 \quad \text{at } y' = 0 \quad (6)$$

$$u' + \eta_1 \frac{\partial u'}{\partial y'} = 0 \quad \text{at } y' = H' = a' + b' \sin \left(\frac{2\pi}{\lambda} (x' - ct') \right) \quad (7)$$

$$\frac{\partial T'}{\partial y'} = 0 \quad \text{at } y' = 0 \quad (8)$$

$$T' + \eta_2 \frac{\partial T'}{\partial y'} = 0 \quad \text{at } y' = H' = a' + b' \sin \left(\frac{2\pi}{\lambda} (x' - ct') \right) \quad (9)$$

where η_1 and η_2 represent velocity and thermal slip parameter respectively.

Constitutive equation of the Sisko fluid model is given as

$$\tau = \left\{ \mu(y) + \beta \left(\frac{\partial u}{\partial y} \right)^{n-1} \right\} \left(\frac{\partial u}{\partial y} \right) \quad (10)$$

where β is the coefficient of pseudo-plasticity, and n is the fluid behaviour index.

Dimensionless quantities of interest are given below

$$\begin{aligned} x &= \frac{x'}{\lambda}, y = \frac{y'}{a'}, u = \frac{u'}{c}, w = \frac{\lambda w'}{ca}, \tau_{xx} = \frac{a' \tau'_{x'x'}}{c \mu}, \tau_{xy} = \frac{a' \tau'_{x'y'}}{c \mu}, \tau_{yy} = \frac{a' \tau'_{y'y'}}{c \mu}, t = \frac{c t'}{\lambda}, \\ Re &= \frac{a c \rho}{\mu}, p = \frac{a'^2 p'}{c \lambda \mu}, \theta = \frac{T' - T'_0}{T_1 - T_0}, Pr = \frac{\mu C_p}{k_1}, \delta = \frac{a'}{\lambda}, \epsilon = \frac{b'}{a'}, F_1 = \frac{\mu c}{\rho g a'}, E_1 = \frac{-\sigma a'^3}{\lambda^3 \mu c}, \\ E_2 &= \frac{m a'^3 c}{\lambda^3 \mu}, E_3 = \frac{a'^3 c}{\lambda^3 \mu}, h = \frac{H'}{a'} = 1 + \epsilon \sin(2\pi(x - t)), \end{aligned} \quad (11)$$

On utilizing the non-dimensional transformations from Eq. (11) in Eq. (2) to Eq. (9), after applying the long wavelength and small Reynolds number approximation, dimensionless governing equations are obtained as

$$\frac{\partial \tau}{\partial y} = \left(\frac{\partial p}{\partial x} \right) - \frac{\sin \gamma}{F} \quad (12)$$

$$\frac{\partial p}{\partial y} = 0 \quad (13)$$

$$\frac{\partial}{\partial y} \left\{ k(\theta) \frac{\partial \theta}{\partial y} \right\} + Br \tau \frac{\partial u}{\partial y} = 0 \quad (14)$$

where γ is the angle of inclination and Br represent the Brinkman number.

Accordingly, the appropriate dimensionless slip boundary conditions are provided by

$$u + \eta_1 \frac{\partial u}{\partial y} = -1 \text{ at } y = h \quad (15)$$

$$\frac{\partial u}{\partial y} = 0 \text{ at } y = 0 \quad (16)$$

$$\theta + \eta_2 \frac{\partial \theta}{\partial y} = 0 \text{ at } y = h \quad (17)$$

$$\frac{\partial \theta}{\partial y} = 0 \text{ at } y = 0 \quad (18)$$

The variation in viscosity $\mu(y)$ and thermal conductivity $k(\theta)$ are given by

$$\mu(y) = 1 - \alpha_1 y \quad \alpha_1 \ll 1 \quad (19)$$

$$k(\theta) = 1 + \alpha_2 \theta \quad \alpha_2 \ll 1 \quad (20)$$

where α_1 and α_2 are the coefficient of variable viscosity and coefficient of thermal conductivity respectively.

3. Solution Methodology

Consider Eq. (12). Let $P = \frac{\partial p}{\partial x}$ and $f = \frac{\sin \gamma}{F}$. On integrating, following expression is obtained

$$\tau = (P - f)y \quad (21)$$

On comparing Eq. (10) and Eq. (21)

$$(P - f) y = \left\{ 1 - \alpha_1 y + \beta \left(\frac{\partial u}{\partial y} \right)^{n-1} \right\} \left(\frac{\partial u}{\partial y} \right) \quad (22)$$

$$\frac{\partial}{\partial y} \left\{ k(\theta) \frac{\partial \theta}{\partial y} \right\} + Br \left\{ (1 - \alpha_1 y) \left(\frac{\partial u}{\partial y} \right) + \beta \left(\frac{\partial u}{\partial y} \right)^n \right\} \left(\frac{\partial u}{\partial y} \right) = 0 \quad (23)$$

The above Eq. (22) and Eq. (23) are non-linear in nature and hence analytical solution for these are tedious. Hence, we introduce the series solution using perturbation technique to obtain the solutions. The solution for stream function (ψ) is obtained in closed form.

3.1 Perturbation Technique

To solve the velocity and temperature expression, the series perturbation technique is applied by using the equations below

$$u = \sum \beta^n u_n \quad (24)$$

$$\theta = \sum \beta^n \theta_n \quad (25)$$

By ignoring $O(\beta^2)$ terms in Eq. (24), expression the for velocity is obtained as

$$u = u_0 + \beta u_1 \quad (26)$$

The zeroth order velocity equation, along with boundary conditions, is given by

$$(P - f) y = \{1 - \alpha_1 y\} \left(\frac{\partial u_0}{\partial y} \right) \quad (27)$$

$$\frac{\partial u_0}{\partial y} = 0 \quad \text{at } y = 0 \quad \text{and} \quad u_0 + \eta_1 \frac{\partial u_0}{\partial y} = -1 \quad \text{at } y = h$$

First order velocity equation with boundary conditions is given by

$$(1 - \alpha_1 y) \left(\frac{\partial u_1}{\partial y} \right) + \left(\frac{\partial u_0}{\partial y} \right)^n = 0 \quad (28)$$

$$\frac{\partial u_1}{\partial y} = 0 \quad \text{at } y = 0 \quad \text{and} \quad u_1 + \eta_1 \frac{\partial u_1}{\partial y} = 0 \quad \text{at } y = h$$

On ignoring $O(\beta^2)$ terms, the expression for temperature is considered as

$$\theta = \theta_0 + \beta \theta_1 \quad (29)$$

Zeroth order temperature expression with boundary conditions is given by

$$\frac{\partial \theta_0}{\partial y} + \alpha_2 \theta_0 \frac{\partial \theta_0}{\partial y} + \int Br \left\{ (1 - \alpha_1 y) \left(\frac{\partial u_0}{\partial y} \right)^2 \right\} \partial y = 0 \quad (30)$$

$$\frac{\partial \theta_0}{\partial y} = 0 \quad \text{at } y = 0 \quad \text{and} \quad \theta_0 + \eta_2 \frac{\partial \theta_0}{\partial y} = 1 \quad \text{at } y = h$$

First order temperature expression with boundary conditions is given by

$$\frac{\partial \theta_1}{\partial y} + \alpha_2 \theta_0 \frac{\partial \theta_1}{\partial y} + \alpha_2 \theta_1 \frac{\partial \theta_0}{\partial y} + \int Br \left\{ 2(1 - \alpha_1 y) \left(\frac{\partial u_0}{\partial y} \right) \left(\frac{\partial u_1}{\partial y} \right) + \beta \left(\frac{\partial u_0}{\partial y} \right)^{n+1} \right\} \partial y = 0 \quad (31)$$

$$\frac{\partial \theta_1}{\partial y} = 0 \quad \text{at } y = 0 \quad \text{and} \quad \theta_1 + \eta_2 \frac{\partial \theta_1}{\partial y} = 0 \quad \text{at } y = h$$

The above equations are non-linear in nature and hence we apply double perturbation technique to obtain the solutions.

$$u_i = \Sigma \alpha_1^j u_{ij}, \text{ where } i = \{0,1\}, 0 \leq j \leq n \quad (32)$$

$$\theta_i = \Sigma \alpha_2^j \theta_{ij}, \text{ where } i = \{0,1\}, 0 \leq j \leq n \quad (33)$$

To obtain simpler solutions for velocity and temperature, higher order terms are ignored, i.e., $O(\alpha_1^2)$ and $O(\alpha_2^2)$. Then the following equations are obtained for velocity and temperature.

$$u_0 = u_{00} + \alpha_1 u_{01} \quad (34)$$

$$u_1 = u_{10} + \alpha_1 u_{11} \quad (35)$$

$$\theta_0 = \theta_{00} + \alpha_2 \theta_{01} \quad (36)$$

$$\theta_1 = \theta_{10} + \alpha_2 \theta_{11} \quad (37)$$

Substituting Eq. (34) in Eq. (27)

Zeroth order velocity equation along with boundary conditions is obtained as

$$u'_{00} = (P - f) y$$

$$\frac{\partial u_{00}}{\partial y} = 0 \text{ at } y = 0 \quad \text{and} \quad u_{00} + \eta_1 \frac{\partial u_{00}}{\partial y} = -1 \text{ at } y = h \quad (38)$$

First order velocity equation along with boundary conditions is obtained as

$$u'_{01} - u'_{00} y = 0$$

$$\frac{\partial u_{01}}{\partial y} = 0 \text{ at } y = 0 \quad \text{and} \quad u_{01} + \eta_1 \frac{\partial u_{01}}{\partial y} = 0 \text{ at } y = h \quad (39)$$

Substituting Eq. (35) in Eq. (28)

Zeroth order velocity equation along with boundary conditions is obtained as

$$u'_{10} + (u'_{00})^n = 0$$

$$\frac{\partial u_{10}}{\partial y} = 0 \text{ at } y = 0 \quad \text{and} \quad u_{10} + \eta_1 \frac{\partial u_{10}}{\partial y} = 0 \text{ at } y = h \quad (40)$$

First order velocity equation along with boundary conditions is obtained as

$$u'_{11} - u'_{10} y + {}^n C u'_{01} (u'_{00})^{n-1} = 0$$

$$\frac{\partial u_{11}}{\partial y} = 0 \text{ at } y = 0 \quad \text{and} \quad u_{11} + \eta_1 \frac{\partial u_{11}}{\partial y} = 0 \text{ at } y = h \quad (41)$$

By solving Eq. (38), Eq. (39), Eq. (40) and Eq. (41) analytically, the expression for velocity is obtained by substituting in Eq. (26).

$$\text{i.e., } u = u_{00} + \alpha_1 u_{01} + \beta u_{10} + \beta \alpha_1 u_{11}$$

The analytical solution for stream function can be obtained by using the equation $u = \frac{\partial \psi}{\partial y}$.

Similarly using Eq. (36) in Eq. (30)

Zeroth order temperature expression along with boundary conditions is obtained as

$$\begin{aligned} \frac{\partial \theta_{00}}{\partial y} + \int Br \left\{ (1 - \alpha_1 y) \left(\frac{\partial u_0}{\partial y} \right)^2 \right\} \partial y &= 0 \\ \frac{\partial \theta_{00}}{\partial y} = 0 \text{ at } y = 0 \text{ and } \theta_{00} + \eta_2 \frac{\partial \theta_{00}}{\partial y} = 1 \text{ at } y = h \end{aligned} \quad (42)$$

First order temperature expression along with boundary conditions is obtained as

$$\begin{aligned} \frac{\partial \theta_{01}}{\partial y} + \theta_{00} \frac{\partial \theta_{00}}{\partial y} &= 0 \\ \frac{\partial \theta_{01}}{\partial y} = 0 \text{ at } y = 0 \text{ and } \theta_{01} + \eta_2 \frac{\partial \theta_{01}}{\partial y} = 0 \text{ at } y = h \end{aligned} \quad (43)$$

Substituting Eq. (37) in Eq. (31)

Zeroth order temperature expression along with boundary conditions is obtained as

$$\begin{aligned} \frac{\partial \theta_{10}}{\partial y} + \int Br \left\{ 2(1 - \alpha_1 y) \left(\frac{\partial u_0}{\partial y} \right) \left(\frac{\partial u_1}{\partial y} \right) + \beta \left(\frac{\partial u_0}{\partial y} \right)^{n+1} \right\} \partial y &= 0 \\ \frac{\partial \theta_{10}}{\partial y} = 0 \text{ at } y = 0 \text{ and } \theta_{10} + \eta_2 \frac{\partial \theta_{10}}{\partial y} = 0 \text{ at } y = h \end{aligned} \quad (44)$$

First order temperature expression along with boundary conditions is obtained as

$$\begin{aligned} \frac{\partial \theta_{11}}{\partial y} + \theta_{00} \frac{\partial \theta_{10}}{\partial y} + \theta_{10} \frac{\partial \theta_{00}}{\partial y} &= 0 \\ \frac{\partial \theta_{11}}{\partial y} = 0 \text{ at } y = 0 \text{ and } \theta_{11} + \eta_2 \frac{\partial \theta_{11}}{\partial y} = 0 \text{ at } y = h \end{aligned} \quad (45)$$

By solving Eq. (42), Eq. (43), Eq. (44) and Eq. (45) analytically, and substituting in Eq. (29) expression for temperature function is obtained as

$$\text{i.e., } \theta = \theta_{00} + \alpha_2 \theta_{01} + \beta \theta_{10} + \beta \alpha_2 \theta_{11}$$

where

$$\frac{\partial p}{\partial x} = P = E_1 \frac{\partial^3 h}{\partial x^3} + E_2 \frac{\partial^3 h}{\partial x \partial t^2} + E_3 \frac{\partial^2 h}{\partial x \partial t} \text{ at } y = h \quad (46)$$

4. Graphical Results and Discussion

The investigation is carried out to examine the influence of fluid parameter (β), coefficient of variable viscosity (α_1), coefficient of variable thermal conductivity (α_2), angle of inclination (γ), Brinkman number (Br) and wall properties E_i ($i = 1, 2, 3$), for velocity (u), temperature (θ) and stream lines (ψ) which are analysed and discussed through graphs. MATLAB 2022a programming is used to calculate the impact of the above parameter with the help of graphs.

4.1 Velocity Profiles

The aim of this subsection is to demonstrate the impact of important components perceived in Figure 2(a)-(e) and Figure 3(a)-(e) on the velocity profile for different fluid behaviour index, say $n = 1$ and $n = 2$ respectively. The figures indicate that the curves are parabolic in all circumstances, with the peak value observed in the centre of the channel. Figure 2(a) represent the fluid parameter of the Sisko fluid for $n = 1$. As the fluid parameter (β) grows, the velocity profile decreases. For an increase in variable viscosity, a rise in velocity profile is noticed (Figure 2(b)). Figure 2(c) depicts the velocity profile for variation in velocity slip parameter. The figure shows an enhancement in the velocity profile for velocity slip parameter. Figure 2(d) represents the variation in inclination angle, which improves the velocity profile as the angle of inclination increases. Figure 2(e) are sketched to observe the change in fluid velocity due to varying wall properties. An increase in velocity profiles can be seen for an increase in wall rigidity and wall elasticity parameters. As the wall damping parameter increases, the velocity profiles also decrease.

Figure 3 represents the variation in velocity profiles for $n = 2$. The fluid parameter of the Sisko fluid is depicted in Figure 3 (a). The velocity profile grows as the fluid parameter increases. Figure 3(b) shows that as the variable viscosity increases, so does the velocity profile. Figure 3(c) depicts an improvement in the velocity profile for the velocity slip parameter. Figure 3(d) depicts the inclination angle fluctuation, which improves the velocity profile as the angle of inclination increases. Figure 3(e) depicts the variation in velocity caused by various wall characteristics. An increase in wall rigidity and elasticity parameters causes an increase in the velocity profile. The velocity profiles decrease as the wall damping parameter rises. This shows that wall properties plays an significant role in the peristalsis.

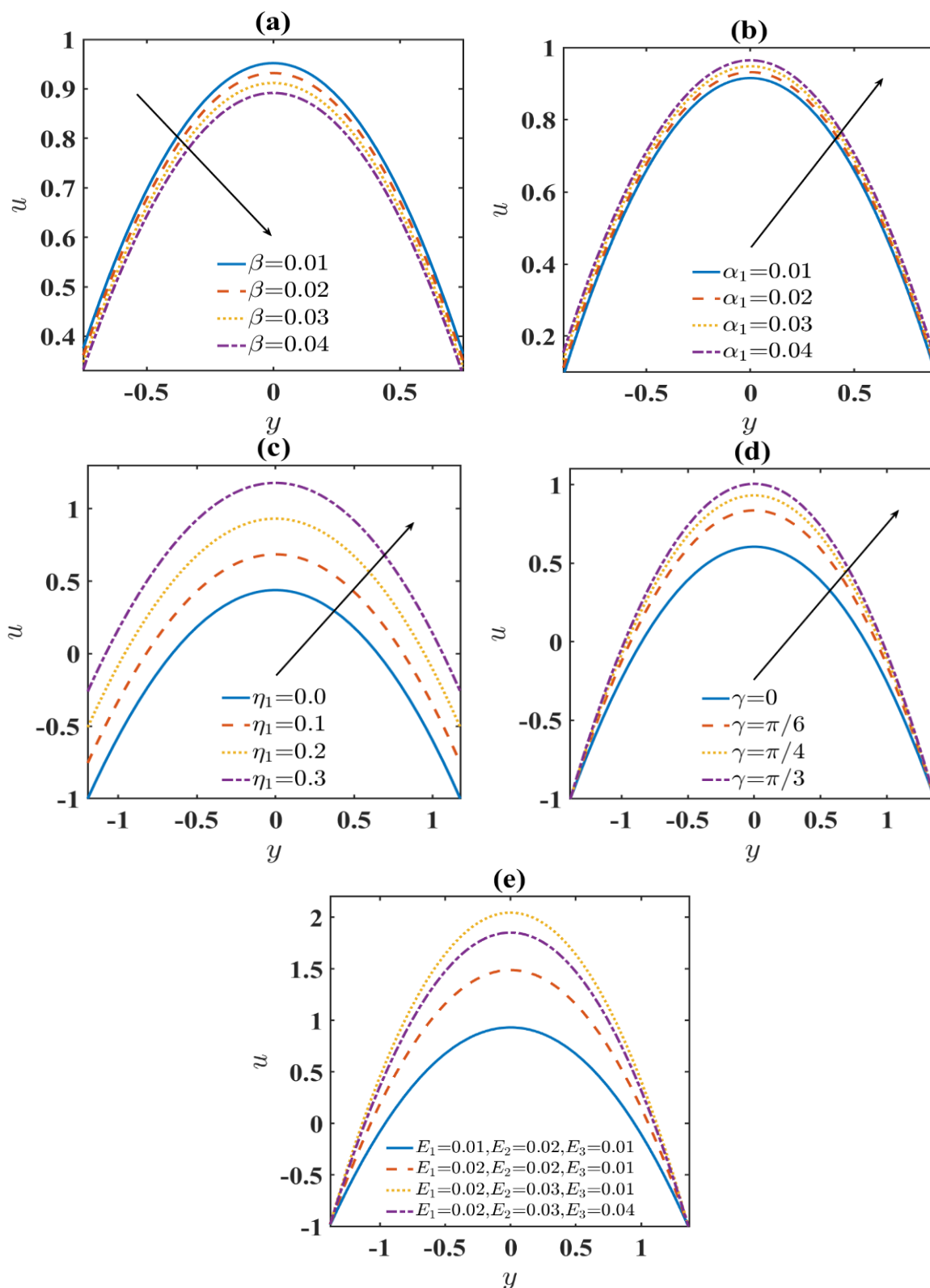


Fig. 2. Variation of velocity profiles when $E_1 = 0.01, E_2 = 0.02, E_3 = 0.01, \beta = 0.02, x = 0.2, F = 2, \eta_1 = 0.2, \gamma = \frac{\pi}{4}, \alpha_1 = 0.02, t = 0.1, \epsilon = 0.3, n = 1$

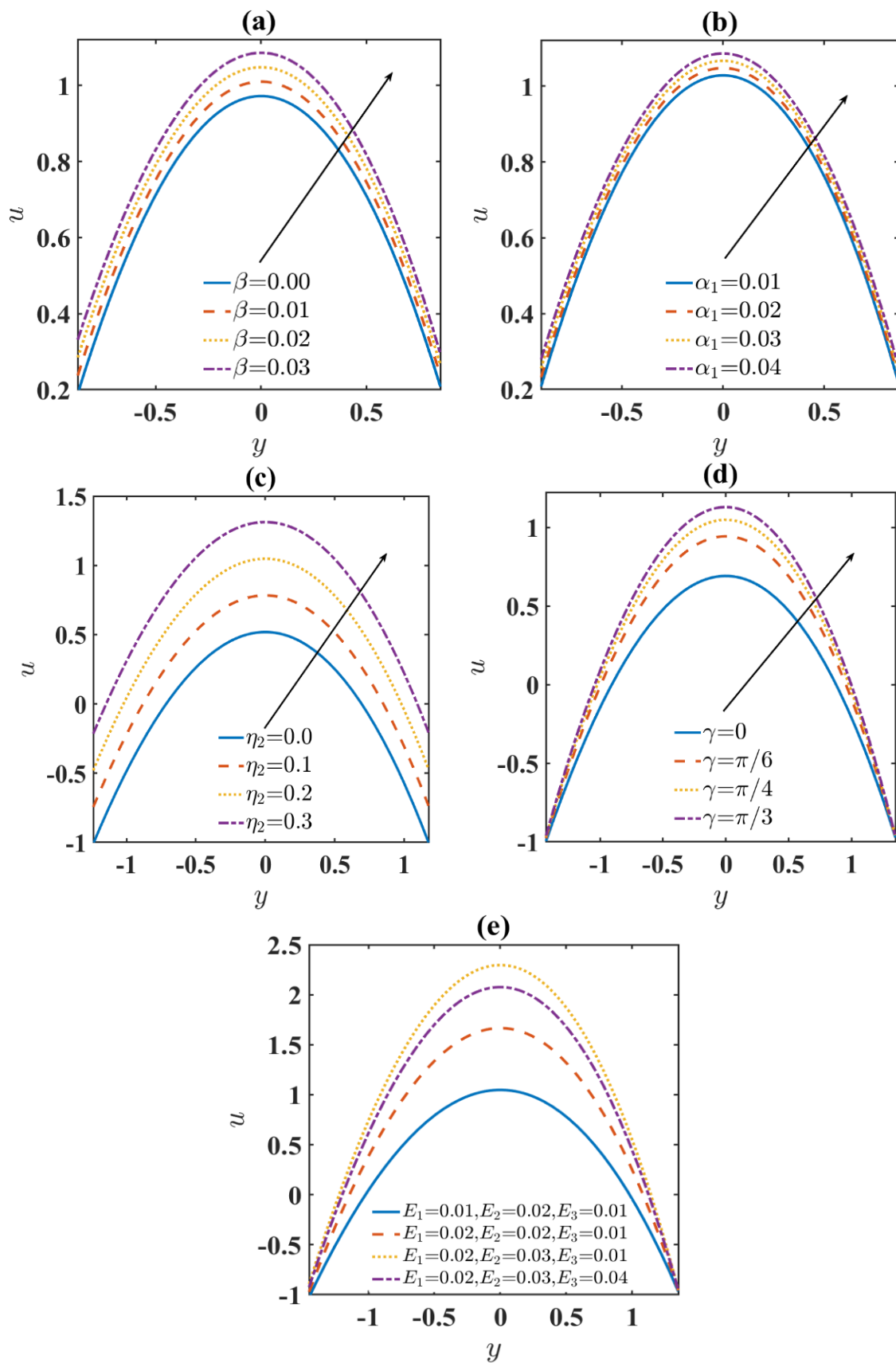
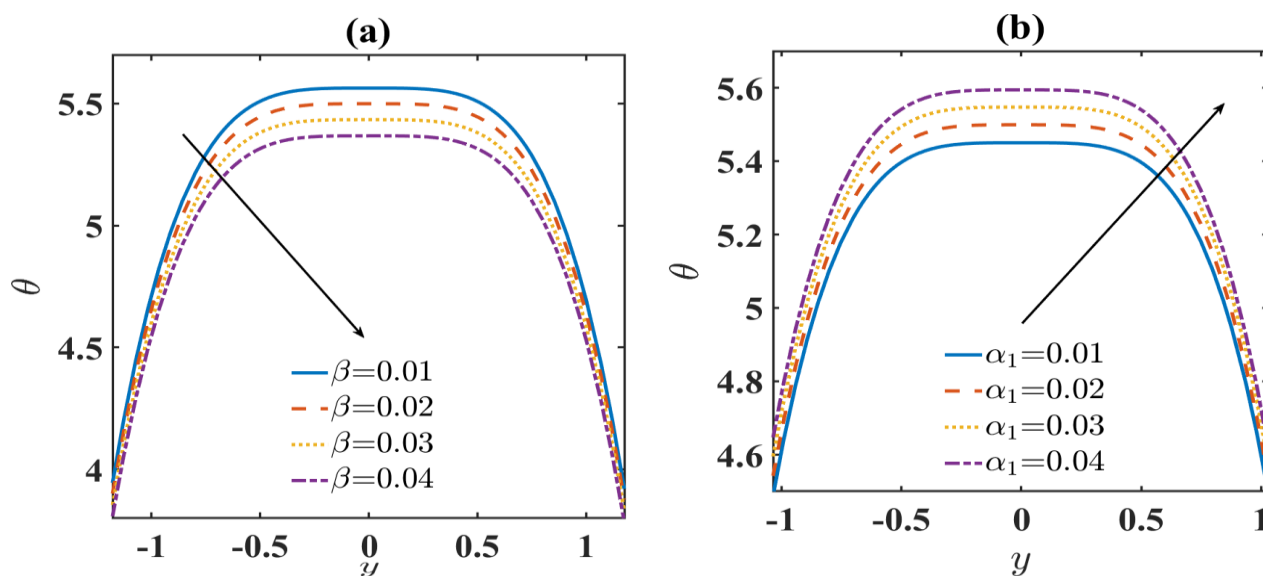


Fig. 3. Variation of velocity profiles when $E_1 = 0.01, E_2 = 0.02, E_3 = 0.01, \beta = 0.02, x = 0.2, F = 2, \eta_1 = 0.2, \gamma = \frac{\pi}{4}, \alpha_1 = 0.02, t = 0.1, \epsilon = 0.3, n = 2$

4.2 Temperature Profiles

The physical description of temperature variation concerning parameter variation in both circumstances is presented in this subsection. The temperature at the wall is lower than that in the centre of the channel and remains constant for all parameter values. This is due to the viscous dissipation effect that favours heat flux. Figure 4(a)-(g) and Figure 5(a)-(g) are drawn for the variation of different parameters for temperature with $n = 1$ and $n = 2$ respectively. Figure 4(a) represent the fluid parameter of the Sisko fluid. As the fluid parameter β increases, temperature profiles decrease for $n = 1$. An increase in the coefficient of variable viscosity increases the temperature while the rise in variable thermal conductivity enhances the temperature, as seen in Figure 4(b) and Figure 4(c) respectively. Figure 4(d) and Figure 4(e), depict the temperature variation for the thermal slip parameter and angle of inclination and both the graphs shows the similar behaviour for temperature. The rise in both thermal slip parameter and inclination angle improves the temperature profiles. An enhancement in temperature profile is seen for the increase in Brinkmann number (See Figure 4(f)). Figure 4(g) shows the plot for varying wall properties. An increase in wall rigidity and elasticity parameters increases the temperature while the damping parameter shows opposite behaviour. These figures clearly show that an increase in wall damping parameter decreases the temperature profiles.



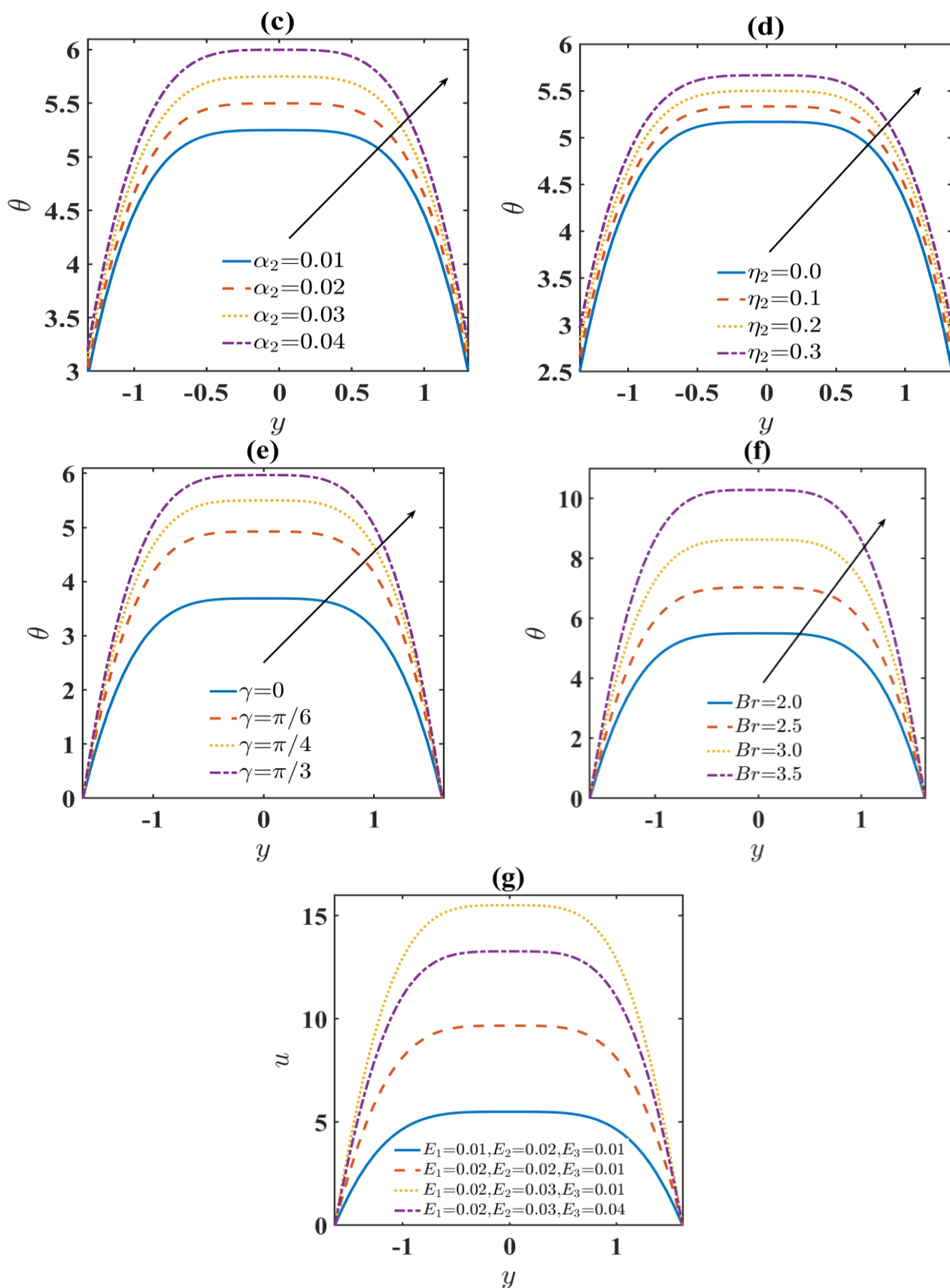
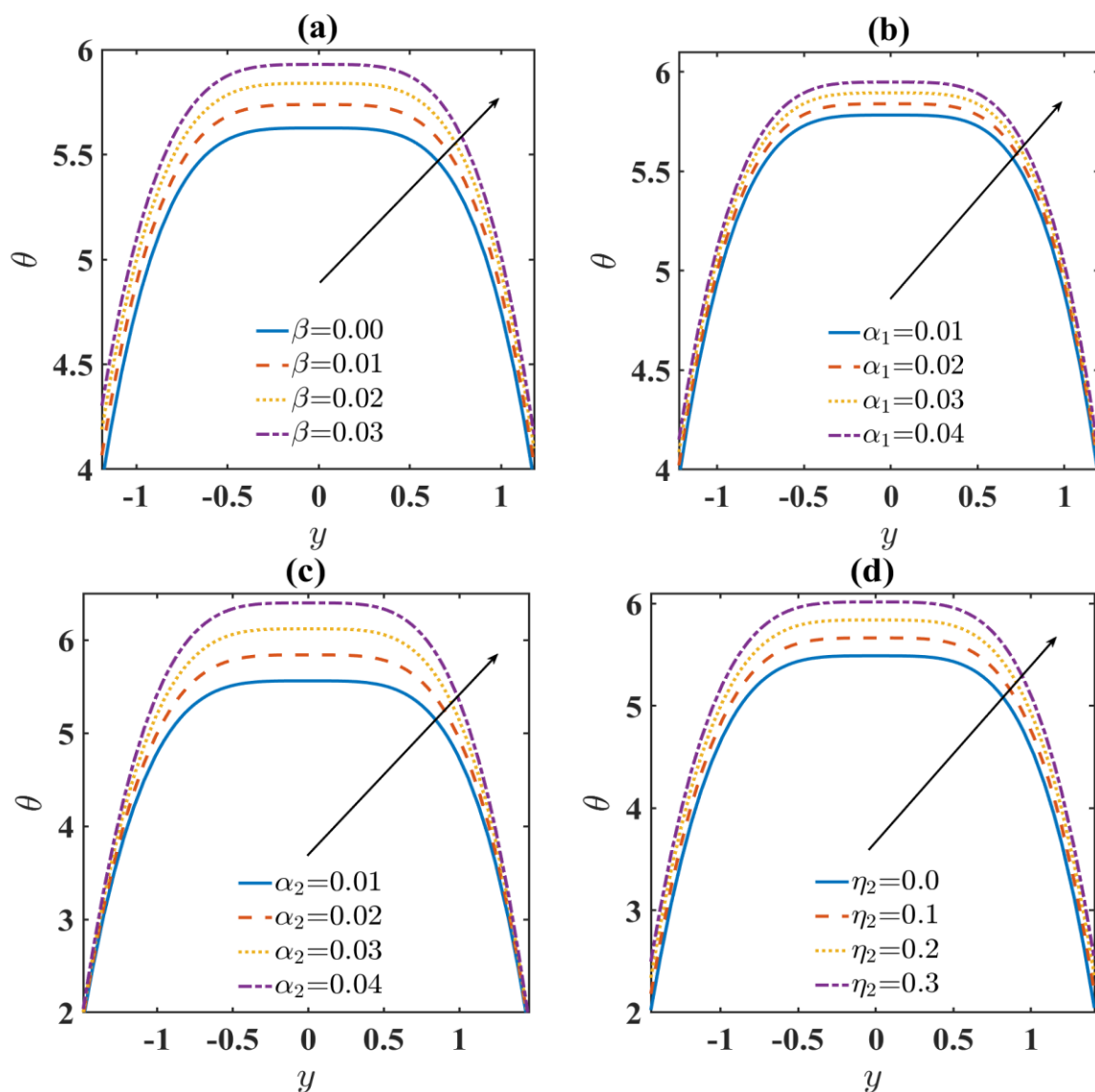


Fig. 4. Variation of temperature profiles when $E_1 = 0.01, E_2 = 0.02, E_3 = 0.01, \beta = 0.02, x = 0.2, F = 2, \eta_2 = 0.2, \gamma = \frac{\pi}{4}, \alpha_1 = 0.02, \alpha_2 = 0.02, t = 0.1, \epsilon = 0.3, Br = 2, n = 1$

Figure 5(a) depicts the fluid parameter of the Sisko fluid. Temperature profiles for $n = 2$ increase as the fluid parameter rises. Temperature rises in response to increases in the coefficient of variable viscosity and variable thermal conductivity, as shown in Figure 5(b) and Figure 5(c). The temperature variation for the thermal slip parameter and angle of inclination are shown in Figure 5(d) and Figure 5(e), respectively, and both graphs exhibit almost the same behaviour for temperature. Temperature profiles are enhanced by improvements in the thermal slip parameter and inclination angle. The temperature profile improves as the Brinkmann number increases (see Figure 5(f)). The plot for different wall characteristics is shown in Figure 5(g). The temperature rises as the wall rigidity and elasticity parameters are increased, whereas the damping parameter exhibits the opposite behaviour. These graphs clearly illustrate that increasing the wall damping value reduces the temperature profiles.



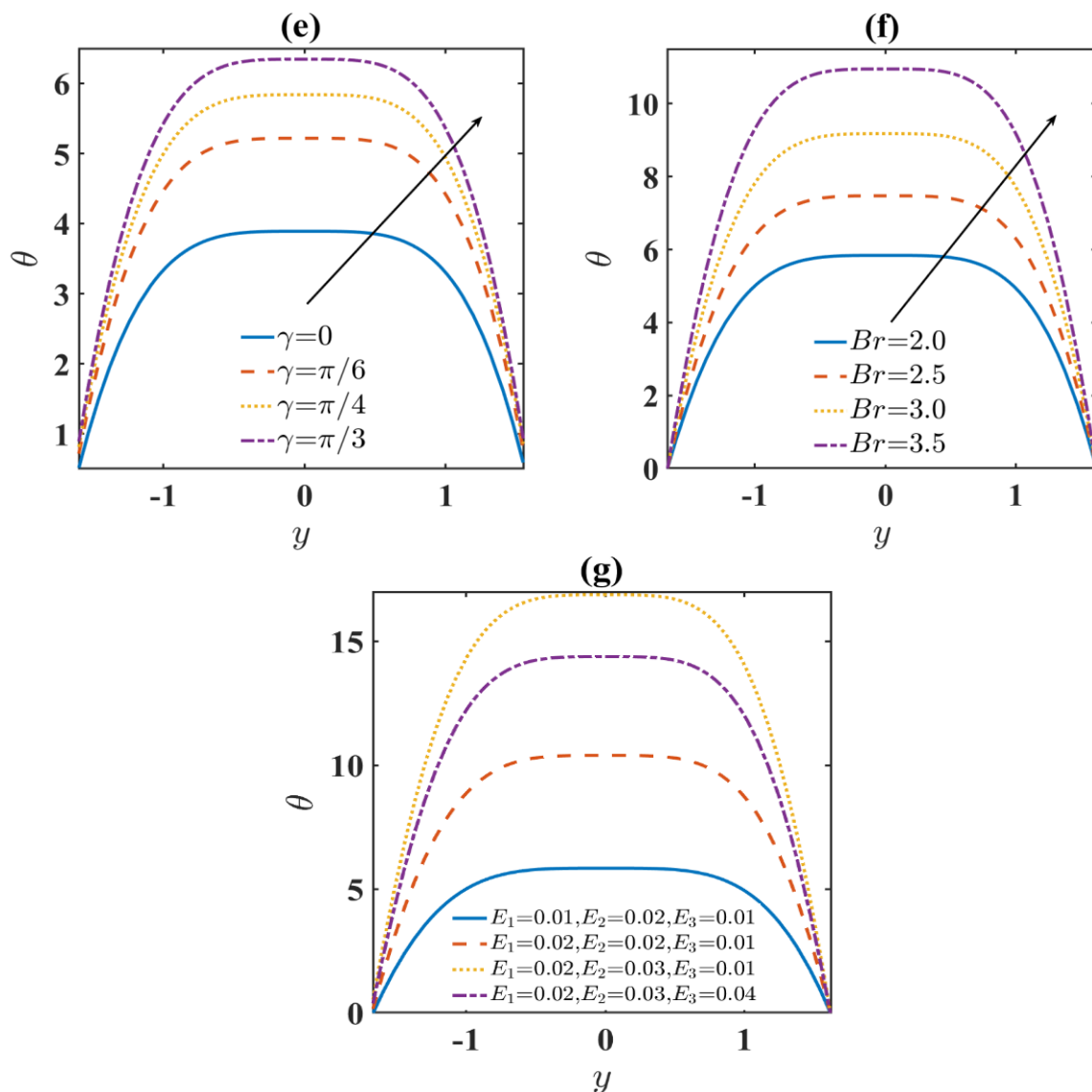


Fig. 5. Variation of temperature profiles when $E_1 = 0.01, E_2 = 0.02, E_3 = 0.01, \beta = 0.02, x = 0.2, F = 2, \eta_2 = 0.2, \gamma = \frac{\pi}{4}, \alpha_1 = 0.02, \alpha_2 = 0.02, t = 0.1, \epsilon = 0.3, Br = 2, n = 2$

4.3 Trapping Phenomenon

Trapping is the most important phenomenon in peristalsis. During peristalsis, a few of its streamlines close, resulting in the formation of boluses that circulate internally and travel forward at the speed of the peristaltic wave. This subsection produced the streamline pattern variation for the considered geometry. These streamlines are depicted in Figure 6 to Figure 10 for $n = 1$ and figure 11-15 for $n = 2$. Figure 6 interprets streamline variation for different values of fluid parameter β . The number of bolus decreases for $n = 1$. Figure 7 depicts the streamlines for variation of coefficient of variable viscosity. As variable viscosity increases, the bolus size also increases. Similar effect is seen in case of velocity slip parameter in Figure 8. The number of formation of boluses increases for increase in angle of inclination for $n = 1$ (See Figure 9). Figure 10 shows the streamlines for different wall properties. It can be noticed that as the wall rigidity parameter increases, there is an increase in the size of the bolus, as seen in 10(b). From 10(b) to 10(c), the number of bolus increases. It is due to the rise in wall elasticity parameters. But in 10(d), the bolus size diminishes for a rise in the wall damping parameter.

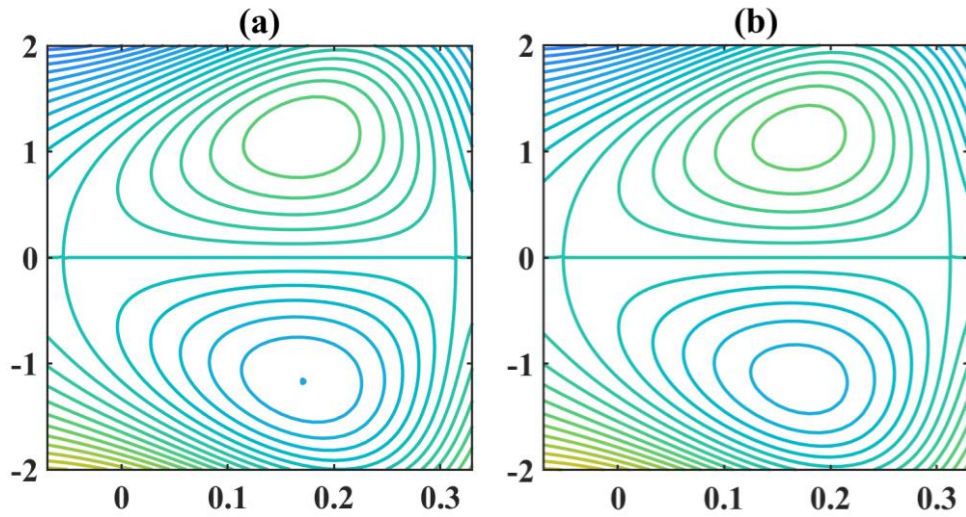


Fig. 6. Variation of streamlines for (a) $\beta = 0.01$, (b) $\beta = 0.04$ for $n = 1$

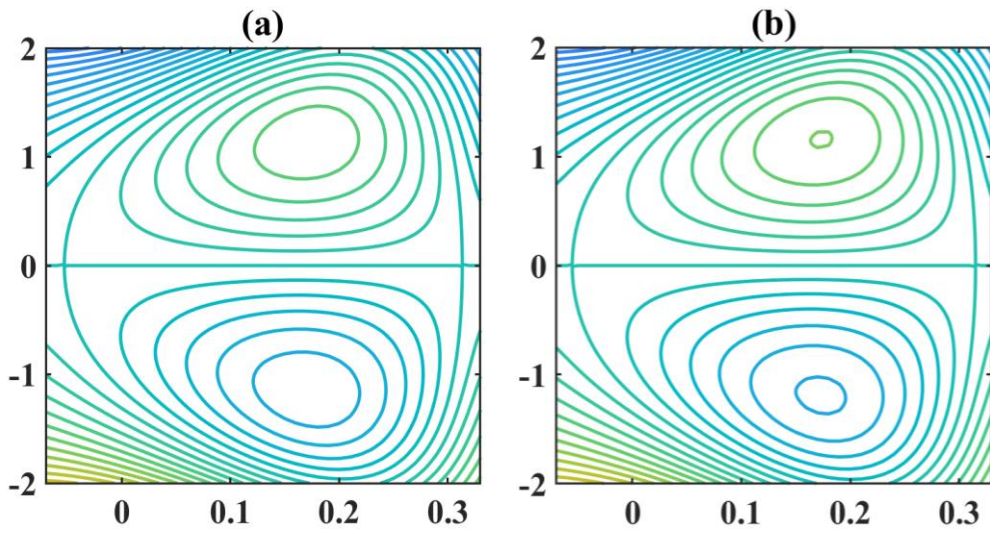


Fig. 7. Variation of streamlines for (a) $\alpha_1 = 0.01$, (b) $\alpha_1 = 0.04$ for $n = 1$

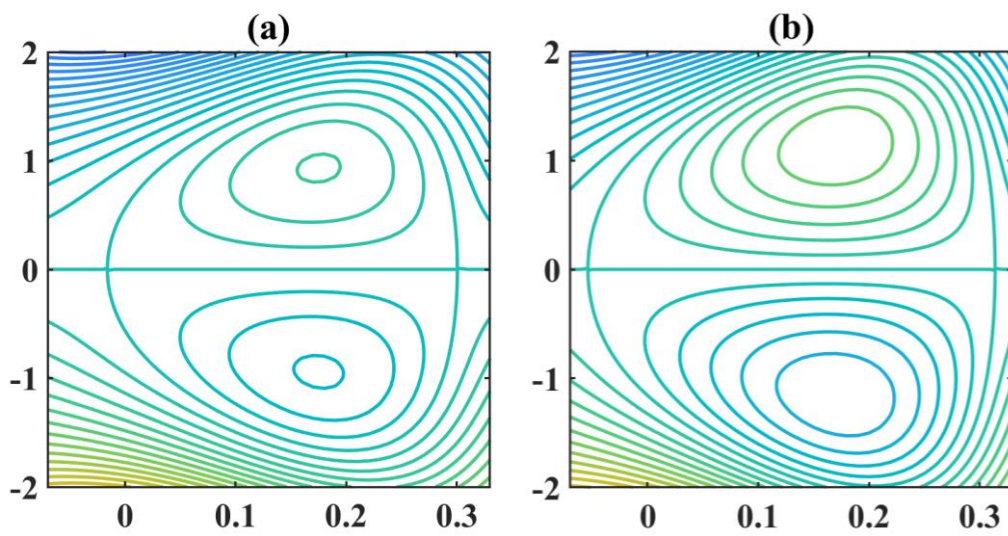


Fig. 8. Variation of streamlines for (a) $\eta_1 = 0.2$, (b) $\eta_1 = 0.4$ for $n = 1$

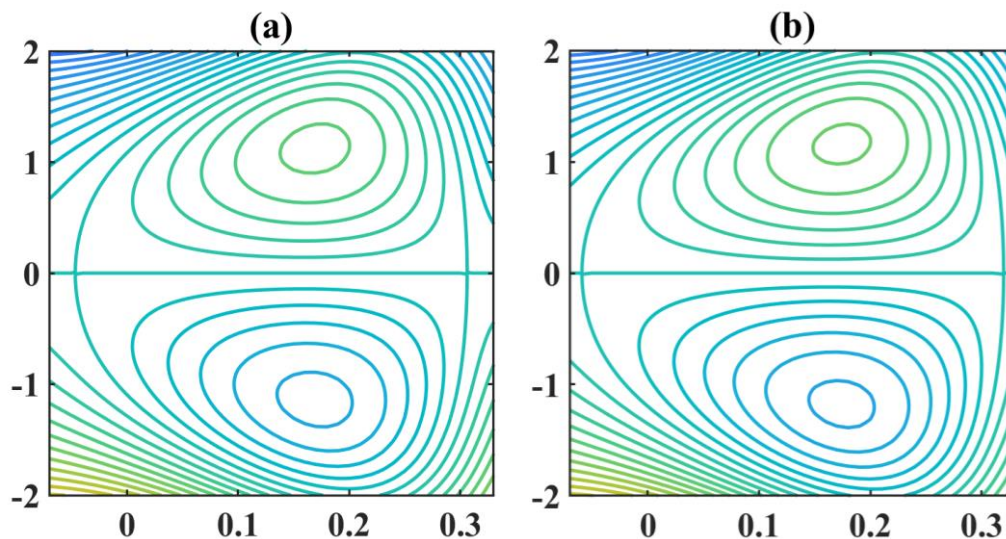


Fig. 9. Variation of streamlines for (a) $\gamma = \pi/6$, (b) $\gamma = \pi/3$ for $n = 1$

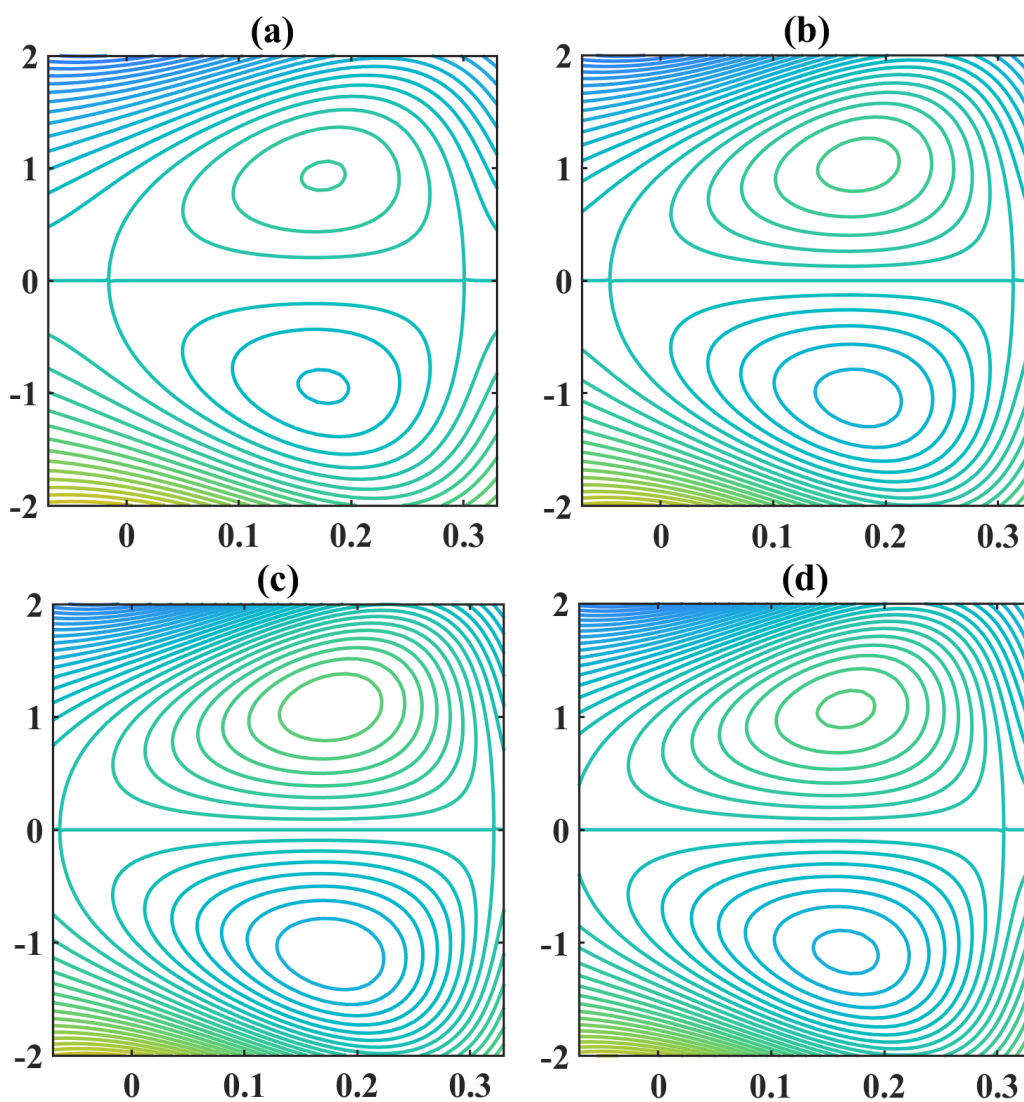


Fig. 10. Variation of streamlines for (a) $E_1 = 0.01, E_2 = 0.02, E_3 = 0.01$ (b) $E_1 = 0.02, E_2 = 0.02, E_3 = 0.01$ (c) $E_1 = 0.02, E_2 = 0.03, E_3 = 0.01$ (d) $E_1 = 0.02, E_2 = 0.03, E_3 = 0.04$ for $n = 1$

Figure 11 depicts the interpretation of streamline variation for various fluid parameter values. For $n = 2$, the number of boluses increases. Figure 12 displays the streamlines for varying the coefficient of variable viscosity. The bolus size grows along with the rise in variable viscosity. The streamlines for the velocity slip parameter are shown in Figure 13. The number of boluses produced is increasing. The number of boluses formed grows as the angle of inclination increases for $n = 2$ (see Figure 14). The streamlines for various wall characteristics are shown in Figure 15. It is evident that the size of the bolus grows as the wall rigidity parameter rises, as shown in Figure 15(b). The number of boluses rises from Figure 15(b) to Figure 15(c). It is caused by increased wall elasticity properties. However, in Figure 15(d), as the wall damping value is increased, the size of the bolus shrinks.

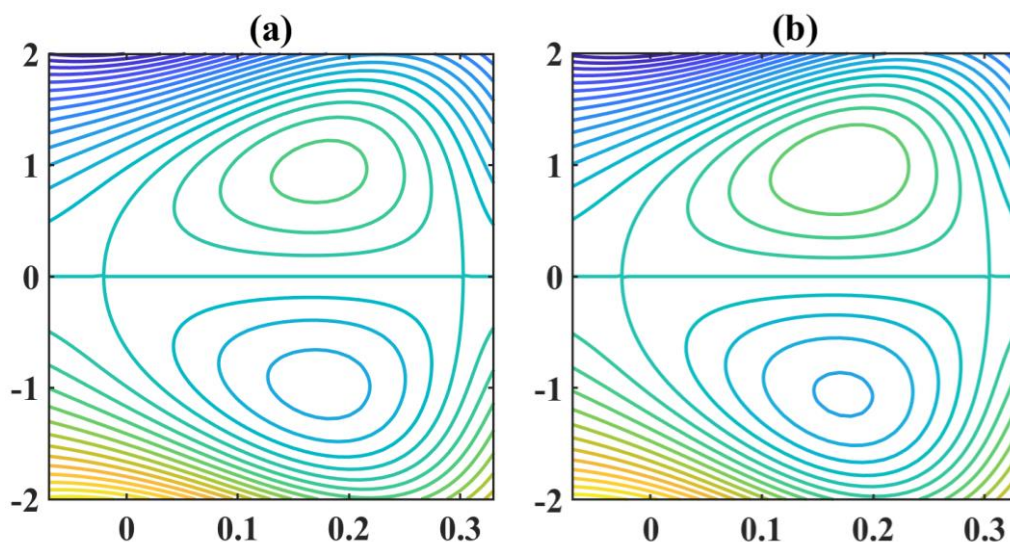


Fig. 11. Variation of streamlines for (a) $\beta = 0.01$, (b) $\beta = 0.04$ for $n = 2$

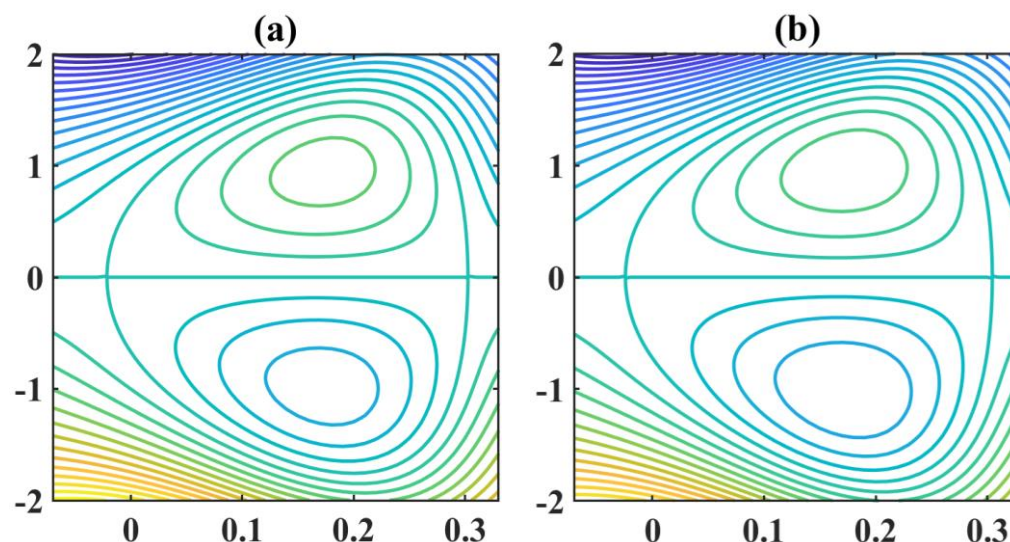


Fig. 12. Variation of streamlines for (a) $\alpha_1 = 0.01$, (b) $\alpha_1 = 0.04$ for $n = 2$

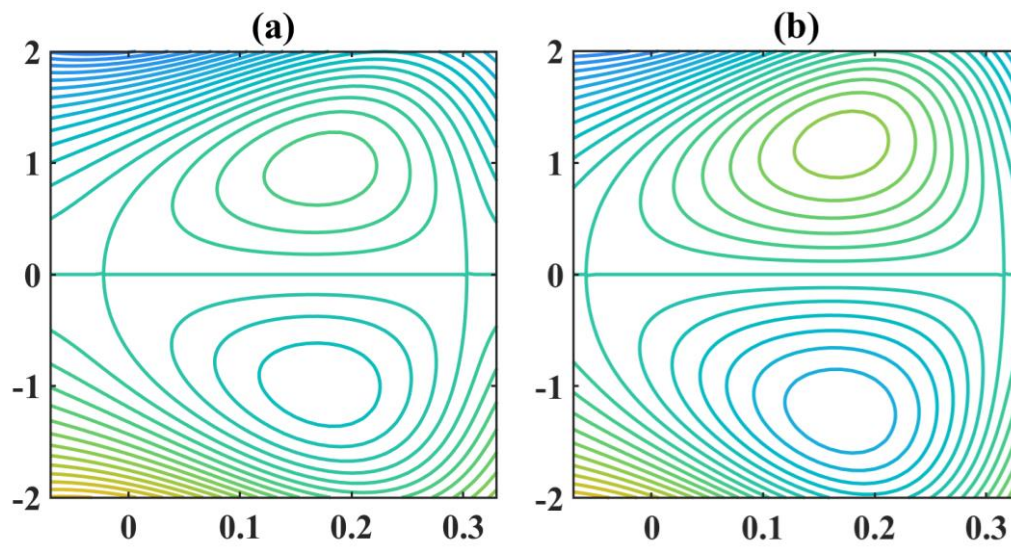


Fig. 13. Variation of streamlines for (a) $\eta_1 = 0.2$, (b) $\eta_1 = 0.4$ for $n = 2$

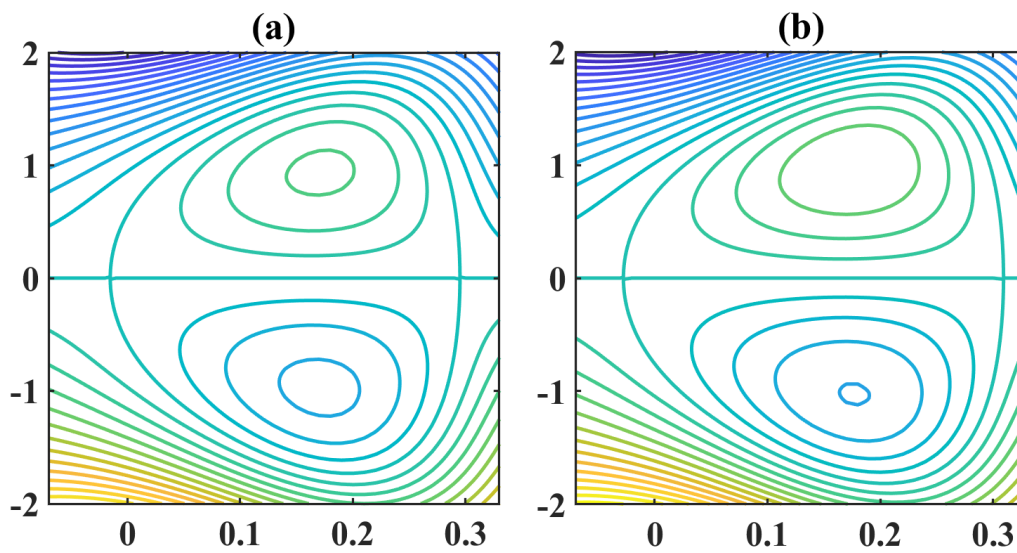


Fig. 14. Variation of streamlines for (a) $\gamma = \pi/6$, (b) $\gamma = \pi/3$ for $n = 2$

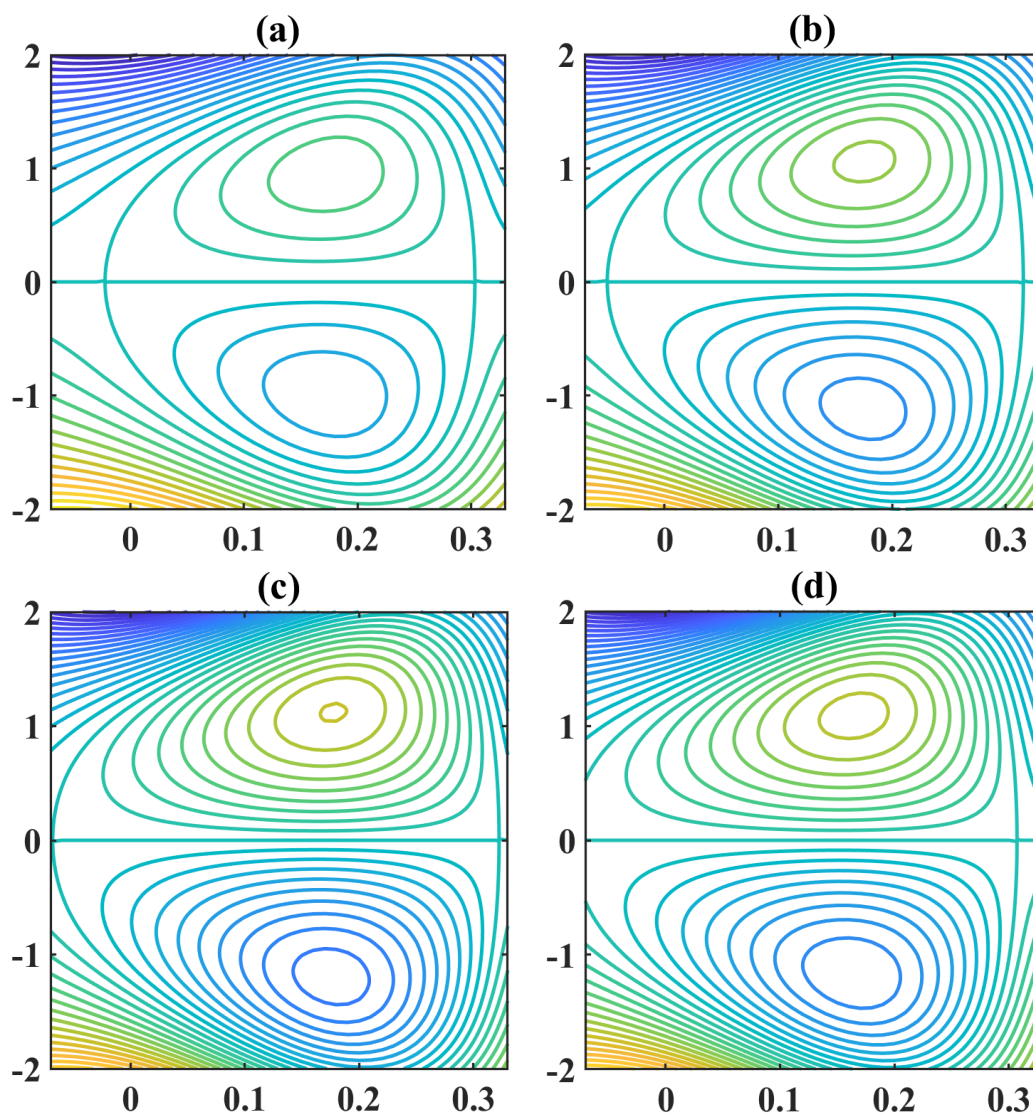


Fig. 15. Variation of streamlines for (a) $E_1 = 0.01, E_2 = 0.02, E_3 = 0.01$ (b) $E_1 = 0.02, E_2 = 0.02, E_3 = 0.01$ (c) $E_1 = 0.02, E_2 = 0.03, E_3 = 0.01$ (d) $E_1 = 0.02, E_2 = 0.03, E_3 = 0.04$ for $n = 2$

5. Conclusion

The peristaltic mechanism of the Sisko fluid is investigated in the current study using a uniform channel by taking variable fluid properties into consideration. Double Perturbation technique is employed to obtain the solution for the governing equations. The objective of the present study is to develop applications in areas such as biomedical engineering, and technology. Some important observations are made during the examination. Preliminary results obtained are as follows

- i. Variable Fluid properties improve the velocity and temperature profiles during peristalsis for both values of $n = 1$ and $n = 2$.
- ii. Velocity slip parameters improves the number of trapped boluses.
- iii. Velocity improves for an increase in wall rigidity and wall elasticity parameters while it declines as wall damping parameter increases.
- iv. Inclination angle increases the velocity and temperature profiles.

References

- [1] Latham, Thomas Walker. "Fluid motions in a peristaltic pump." *PhD diss., Massachusetts Institute of Technology*, 1966.
- [2] Sharpio, A. H., M. Y. Jaffrin, B. R. P. Rao, and S. I. Weinberg. "Peristaltic pumping with long wavelength and low Reynolds number." *Journal of Fluid Mechanics* 37, no. 4 (1969): 799-825. <https://doi.org/10.1017/S0022112069000899>
- [3] Raju, K. Kanaka, and Rathna Devanathan. "Peristaltic motion of a non-Newtonian fluid." *Rheologica Acta* 11, no. 2 (1972): 170-178. <https://doi.org/10.1007/BF01993016>
- [4] Srivastava, L. M., and V. P. Srivastava. "Peristaltic transport of a power-law fluid: application to the ductus efferentes of the reproductive tract." *Rheologica Acta* 27 (1988): 428-433. <https://doi.org/10.1007/BF01332164>
- [5] Srinivas, S., and M. Kothandapani. "Peristaltic transport in an asymmetric channel with heat transfer-a note." *International Communications in Heat and Mass Transfer* 35, no. 4 (2008): 514-522. <https://doi.org/10.1016/j.icheatmasstransfer.2007.08.011>
- [6] Srinivas, S., and M. Kothandapani. "The influence of heat and mass transfer on MHD peristaltic flow through a porous space with compliant walls." *Applied Mathematics and Computation* 213, no. 1 (2009): 197-208. <https://doi.org/10.1016/j.amc.2009.02.054>
- [7] Khan, Ambreen Afsar, Rahmat Ellahi, and Muhammad Usman. "The effects of variable viscosity on the peristaltic flow of non-Newtonian fluid through a porous medium in an inclined channel with slip boundary conditions." *Journal of Porous Media* 16, no. 1 (2013). <https://doi.org/10.1615/JPorMedia.v16.i1.60>
- [8] Gudekote, Manjunatha, and Rajashekhar Choudhari. "Slip effects on peristaltic transport of Casson fluid in an inclined elastic tube with porous walls." *Journal of Advanced Research in Fluid Mechanics and Thermal Sciences* 43, no. 1 (2018): 67-80.
- [9] Gudekote, Manjunatha, Rajashekhar Choudhari, K. V. Prasad, Hanumesh Vaidya, K. Vajravelu, and S. Sreenadh. "Peristaltic pumping of a Casson fluid in a convectively heated porous channel with variable fluid properties." *Journal of Nanofluids* 8, no. 7 (2019): 1446-1457. <https://doi.org/10.1166/jon.2019.1710>
- [10] Prasad, K. V., Hanumesh Vaidya, C. Rajashekhar, Sami Ullah Khan, G. Manjunatha, and J. U. Viharika. "Slip flow of MHD Casson fluid in an inclined channel with variable transport properties." *Communications in Theoretical Physics* 72, no. 9 (2020): 095004. <https://doi.org/10.1088/1572-9494/aba246>
- [11] Baliga, Divya, Manjunatha Gudekote, Rajashekhar Choudhari, Hanumesh Vaidya, and Kerehalli Vinayaka Prasad. "Influence of velocity and thermal slip on the peristaltic transport of a herschel-bulkley fluid through an inclined porous tube." *Journal of Advanced Research in Fluid Mechanics and Thermal Sciences* 56, no. 2 (2019): 195-210.
- [12] Balachandra, H., C. Rajashekhar, F. Mebarek-Oudina, G. Manjunatha, H. Vaidya, and K. V. Prasad. "Slip effects on a ree-eyring liquid peristaltic flow towards an inclined channel and variable liquid properties." *Journal of Nanofluids* 10, no. 2 (2021): 246-258. <https://doi.org/10.1166/jon.2021.1781>
- [13] Khan, Sudheer, and Shu Wang. "An Exploratory Approach to Study Electro-Osmotic of Non-Newtonian Bio-Bi-Phase Flow Due to Peristaltic Transport of Particulate Fluid." *Journal of Advanced Research in Fluid Mechanics and Thermal Sciences* 81, no. 1 (2021): 99-119. <https://doi.org/10.37934/arfmts.81.1.99119>
- [14] Vajravelu, Kuppapalle, G. Radhakrishnamacharya, and V. Radhakrishnamurty. "Peristaltic flow and heat transfer in a vertical porous annulus, with long wave approximation." *International Journal of Non-Linear Mechanics* 42, no. 5 (2007): 754-759. <https://doi.org/10.1016/j.ijnonlinmec.2007.02.014>
- [15] Rajashekhar, C., G. Manjunatha, Hanumesh Vaidya, B. Divya, and K. Prasad. "Peristaltic flow of Casson liquid in an inclined porous tube with convective boundary conditions and variable liquid properties." *Frontiers in Heat and Mass Transfer (FHMT)* 11 (2018). <https://doi.org/10.5098/hmt.11.35>
- [16] Vaidya, Hanumesh, Rajashekhar Choudhari, Manjunatha Gudekote, and Kerehalli Vinayaka Prasad. "Effect of variable liquid properties on peristaltic transport of Rabinowitsch liquid in convectively heated compliant porous channel." *Journal of Central South University* 26, no. 5 (2019): 1116-1132. <https://doi.org/10.1007/s11771-019-4075-x>
- [17] Vaidya, Hanumesh, C. Rajashekhar, G. Manjunatha, and K. V. Prasad. "Rheological properties and peristalsis of Rabinowitsch fluid through compliant porous walls in an inclined channel." *Journal of Nanofluids* 8, no. 5 (2019): 970-979. <https://doi.org/10.1166/jon.2019.1664>
- [18] Manjunatha, G., C. Rajashekhar, Hanumesh Vaidya, K. V. Prasad, and K. Vajravelu. "Impact of heat and mass transfer on the peristaltic mechanism of Jeffery fluid in a non-uniform porous channel with variable viscosity and thermal conductivity." *Journal of Thermal Analysis and Calorimetry* 139 (2020): 1213-1228. <https://doi.org/10.1007/s10973-019-08527-8>
- [19] Khan, Waqar Azeem, Shahid Farooq, S. Kadry, M. Hanif, F. J. Iftikhar, and Syed Zaheer Abbas. "Variable characteristics of viscosity and thermal conductivity in peristalsis of magneto-Carreau nanoliquid with heat transfer

- irreversibilities." *Computer Methods and Programs in Biomedicine* 190 (2020): 105355. <https://doi.org/10.1016/j.cmpb.2020.105355>
- [20] Abuiyada, Alaa Jaber, Nabil Tawfik Eldabe, Mohamed Yahya Abou-zeid, and Sami Mohamed El Shaboury. "Effects of Thermal Diffusion and Diffusion Thermo on a Chemically Reacting MHD Peristaltic Transport of Bingham Plastic Nanofluid." *Journal of Advanced Research in Fluid Mechanics and Thermal Sciences* 98, no. 1 (2022): 24-43. <https://doi.org/10.37934/arfmts.98.1.2443>
- [21] Vaidya, Hanumesh, K. V. Prasad, M. Ijaz Khan, F. Mebarek-Oudina, I. Tlili, C. Rajashekhar, Samia Elattar, Muhammad Imran Khan, and Sami G. Al-Gamdi. "Combined effects of chemical reaction and variable thermal conductivity on MHD peristaltic flow of Phan-Thien-Tanner liquid through inclined channel." *Case Studies in Thermal Engineering* 36 (2022): 102214. <https://doi.org/10.1016/j.csite.2022.102214>
- [22] Wang, Yongqi, Tasawar Hayat, Nasir Ali, and Martin Oberlack. "Magnetohydrodynamic peristaltic motion of a Sisko fluid in a symmetric or asymmetric channel." *Physica A: Statistical Mechanics and its Applications* 387, no. 2-3 (2008): 347-362. <https://doi.org/10.1016/j.physa.2007.10.020>
- [23] Nadeem, Sohail, and Noreen Sher Akbar. "Peristaltic flow of Sisko fluid in a uniform inclined tube." *Acta Mechanica Sinica* 26, no. 5 (2010): 675-683. <https://doi.org/10.1007/s10409-010-0356-1>
- [24] Nadeem, S., Noreen Sher Akbar, and K. Vajravelu. "Peristaltic flow of a Sisko fluid in an endoscope: analytical and numerical solutions." *International Journal of Computer Mathematics* 88, no. 5 (2011): 1013-1023. <https://doi.org/10.1080/00207160.2010.489640>
- [25] Mehmood, Obaid Ullah, and Constantin Fetecau. "A note on radiative heat transfer to peristaltic flow of Sisko fluid." *Applied Bionics and Biomechanics* 2015 (2015). <https://doi.org/10.1155/2015/283892>
- [26] Malik, Rabia, and Masood Khan. "Numerical study of homogeneous-heterogeneous reactions in Sisko fluid flow past a stretching cylinder." *Results in Physics* 8 (2018): 64-70. <https://doi.org/10.1016/j.rinp.2017.10.047>
- [27] Tanveer, A., T. Hayat, and A. Alsaedi. "Variable viscosity in peristalsis of Sisko fluid." *Applied Mathematics and Mechanics* 39 (2018): 501-512. <https://doi.org/10.1007/s10483-018-2313-8>
- [28] Asghar, Zeeshan, Nasir Ali, Raheel Ahmed, Muhammad Waqas, and Waqar Azeem Khan. "A mathematical framework for peristaltic flow analysis of non-Newtonian Sisko fluid in an undulating porous curved channel with heat and mass transfer effects." *Computer Methods and Programs in Biomedicine* 182 (2019): 105040. <https://doi.org/10.1016/j.cmpb.2019.105040>
- [29] Iqbal, Naveed, Humaira Yasmin, Bawfeh K. Kometa, and Adel A. Attiya. "Effects of convection on Sisko fluid with peristalsis in an asymmetric channel." *Mathematical and Computational Applications* 25, no. 3 (2020): 52. <https://doi.org/10.3390/mca25030052>
- [30] Imran, Naveed, Maryam Javed, Muhammad Sohail, and Iskander Tlili. "Utilization of modified Darcy's law in peristalsis with a compliant channel: applications to thermal science." *Journal of Materials Research and Technology* 9, no. 3 (2020): 5619-5629. <https://doi.org/10.1016/j.jmrt.2020.03.087>
- [31] Abbas, Zaheer, Muhammad Yousuf Rafiq, Sabeeh Khaliq, and Amjad Ali. "Dynamics of the thermally radiative and chemically reactive flow of Sisko fluid in a tapered channel." *Advances in Mechanical Engineering* 14, no. 10 (2022): 16878132221129735. <https://doi.org/10.1177/16878132221129735>